Am J Physiol Cell Physiol
281: C908–C921, 2001.

Proton leak and CFTR in regulation of Golgi pH in respiratory epithelial cells

GRISCHA CHANDY,[1] MICHAEL GRABE,[2] HSIAO-PING H. MOORE,[1] AND TERRY E. MACHEN[1]
[1]*Department of Molecular and Cell Biology and* [2]*Department of Physics, University of California, Berkeley, California 94720-3200*

Received 26 October 2000; accepted in final form 16 April 2001

Chandy, Grischa, Michael Grabe, Hsiao-Ping H. Moore, and Terry E. Machen. Proton leak and CFTR in regulation of Golgi pH in respiratory epithelial cells. *Am J Physiol Cell Physiol* 281: C908–C921, 2001.—Work addressing whether cystic fibrosis transmembrane conductance regulator (CFTR) plays a role in regulating organelle pH has remained inconclusive. We engineered a pH-sensitive excitation ratiometric green fluorescent protein (pHERP) and targeted it to the Golgi with sialyltransferase (ST). As determined by ratiometric imaging of cells expressing ST-pHERP, Golgi pH (pH_G) of HeLa cells was 6.4, while pH_G of mutant (ΔF508) and wild-type CFTR-expressing (WT-CFTR) respiratory epithelia were 6.7–7.0. Comparison of genetically matched ΔF508 and WT-CFTR cells showed that the absence of CFTR statistically increased Golgi acidity by 0.2 pH units, though this small difference was unlikely to be physiologically important. Golgi pH was maintained by a H^+ vacuolar (V)-ATPase countered by a H^+ leak, which was unaffected by CFTR. To estimate Golgi proton permeability (P_{H^+}), we modeled transient changes in pH_G induced by inhibiting the V-ATPase and by acidifying the cytosol. This analysis required knowing Golgi buffer capacity, which was pH dependent. Our in vivo estimate is that Golgi $P_{H^+} = 7.5 \times 10^{-4}$ cm/s when pH_G = 6.5, and surprisingly, P_{H^+} decreased as pH_G decreased.

enhanced yellow fluorescent protein; ultraviolet enhanced green fluorescent protein; trachea; organelle pH; proton permeability; cystic fibrosis

CYSTIC FIBROSIS (CF) is the most common fatal genetic disease among Caucasians. CF is caused by mutations in the gene encoding the cystic fibrosis transmembrane conductance regulator (CFTR), which is a cAMP/protein kinase A-regulated Cl^- channel that is absent or defective in CF. CF patients most commonly succumb to respiratory complications that arise because of colonization of the respiratory tract by *Pseudomonas aeruginosa* and other opportunistic bacteria. One hypothesis to explain how a reduction of Cl^- permeability could lead to colonization of CF lungs by *P. aeruginosa* is that pH of the Golgi (pH_G), *trans*-Golgi, and *trans*-Golgi network, which are normally acidic relative to the cytosol, are alkaline in CF. CFTR, which could serve as the counterion conductance, may be required to prevent generation of large lumen-positive membrane voltages during pumping by the electrogenic H^+ vacuolar (V)-ATPase (1, 2). The lack of CFTR would lead to an alkaline pH_G, which in turn would alter the activities of resident enzymes responsible for proper sialylation, sulfation, and fucosylation [due to sialyltransferase (ST), sulfotransferase, and fucosyltransferase, respectively] of secreted and surface membrane components. These alterations could lead to changes in the chemical properties of membrane and secreted glycoproteins and glycolipids, such as increased asialo-GM1, a hypothesized bacterial binding site on epithelia (5, 11, 25, 63) [see also Schroeder et al. (45) for conflicting opinion].

A number of groups have attempted to test the organelle pH hypothesis. Lukacs et al. (33) demonstrated that CFTR was functional in endosomes of Chinese hamster ovary (CHO) cells heterologously expressing CFTR, but they concluded that factors other than CFTR were the major determinants of endosomal pH. Dunn et al. (12) found that endocytic acidification was independent of CFTR when the CF pancreatic cell line (CFPAC) and CFTR-corrected CFPAC cells were compared. Seksek et al. (48) microinjected liposomes containing pH-sensitive fluid-phase dyes into the Golgi of fibroblasts and epithelial cells and found that pH_G was the same in both cell types and also in epithelial cells that normally do (Calu-3) and do not (Madin-Darby canine kidney, SK-MES-1) express CFTR (49).

There were three reasons for performing a rigorous test of the organelle pH hypothesis. First, human airway epithelial cells may be different from fibroblasts, lymphocytes, and non-airway epithelial cells from other species with regard to pH_G regulation. Second, none of the previous comparisons of pH_G was performed on cells that were genetically matched ΔF508 (deletion of Phe-508 in CFTR) and wild-type CFTR-expressing (WT-CFTR) respiratory cell lines. Third, it was important to measure the pH of Golgi cisternae where ST and the other critical enzymes reside because pH regulatory mechanisms may differ in different organelles (54), and none of the other studies had defin-

Address for reprint requests and other correspondence: T. E. Machen, 231 LSA, Univ. of California, Berkeley, CA 94720-3200 (E-mail: machen@socrates.berkeley.edu).

The costs of publication of this article were defrayed in part by the payment of page charges. The article must therefore be hereby marked "*advertisement*" in accordance with 18 U.S.C. Section 1734 solely to indicate this fact.

itively measured pH in the ST-containing region of the Golgi.

We developed a ratiometric, green fluorescent protein (GFP)-based pH sensor that was targeted to the Golgi with ST in genetically matched ΔF508-CF and CFTR-corrected ΔF508-CF human airway epithelial cells. Various pH-sensitive mutants of GFP (pK_a 5–7) have been targeted to the Golgi (as well as mitochondria and endoplasmic reticulum) (28, 32, 55), but artifacts can arise with the use of the single-wavelength intensity changes of these GFPs when the apparent or actual fluorophore concentration changes (e.g., due to bleaching or changes in path length) and pH does not. By fusing ultraviolet enhanced GFP (GFPuv) and enhanced yellow fluorescent protein (EYFP), we created a chimeric protein that has an excitation spectrum with pH-dependent (490 nm) and relatively pH-independent (440 nm) wavelengths. Measurements of pH_G in HeLa cells were used to confirm the method, and measurements in CF (ΔF508 CFTR) tracheal (CFT1) and human nasal epithelial (JME) cells and in CFTR-expressing tracheal (CFT1-CFTR) and human bronchial epithelial (HBE) cells were used to determine the role of CFTR in the control of pH_G.

It was also expected that pH_G would be critically affected by the magnitude of H^+ leaks. Because CFTR may control both Na^+ conductance (29, 39, 50) and anion (Cl^-/HCO_3^-) exchange (31) in the plasma membranes of epithelial cells, it seemed possible that CFTR mutations might also affect pH_G by altering H^+ leak pathways. We therefore compared H^+ leaks in CFT1 and CFT1-CFTR cells. We also developed a mathematical model that used measurements of pH_G, cytosolic pH [pH_C, with the cytosolic dye 2′,7′-bis(2-carboxyethyl)-5(6)-carboxyfluorescein (BCECF)], and buffer capacity of the Golgi to make the first in vivo estimates of Golgi membrane H^+ permeability (P_{H^+}, in cm/s) in CFT1 cells.

METHODS

Materials

All salts, glucose, buffers, dibutyryl-cAMP, adenine, transferrin, insulin, chloroquine, DMSO, triiodothyronine, hydrocortisone, cholera toxin, epithelial growth factor (EGF), epinephrine, endothelial cell growth supplement, DEAE dextran, bafilomycin, nigericin, and monensin were obtained from Sigma (St. Louis, MO); forskolin and sometimes bafilomycin were obtained from Calbiochem (San Diego, CA); solvents were from Fisher Scientific (Pittsburgh, PA); and restriction enzymes were from New England Biolabs (Beverly, MA). Tissue culture reagents were obtained from GIBCO-BRL or Cellgro. Fetal bovine serum (FBS) was obtained from Gemini Bio-Products. BCECF-AM and Pluronic F-127 were from Molecular Probes, (Eugene, OR).

Construction of Plasmids

Bacterial expression vector for pHERP. To create a bacterial expression vector for pH-sensitive excitation ratiometric green fluorescent protein (pHERP), EYFP (S65G, S72A, T203Y, H231L) was PCR-amplified with a sense primer (5′-cccaagcttgatggtgagcaagggcgag-3′) containing a *Hin*dIII restriction site (underlined) and an antisense primer (5′-gacgagctgtacaagggaggaggtctagag-3′) that codes for a linker region. An *Xba*I restriction site (underlined) is present and eliminated the EYFP stop codon. Cloning the product into GFPuv (F99S, M153T, V163A; Clonetech) put EYFP upstream of GFPuv with an intervening linker region having the amino acid sequence GGGLEDPRVPVEK.

ST-pHERP mammalian expression vector. We PCR amplified the ST fragment, amino acids 1–70 containing the cytosolic, transmembrane, and truncated luminal domains, from human 2′,6-sialyltransferase (courtesy of Dr. Brian Seed, Harvard Medical School and Massachusetts General Hospital). This portion of ST has been used to target chimeric molecules to the Golgi (60, 61). PCR amplification was performed with primers (5′-cgcgggaagcttgccaccatgattcacaccaacctg-3′ and 5′-cgcgggcggatcctgggtgctgcttgagga-3′) that allowed cloning of the PCR product into the pcDNA3 vector (Invitrogen, San Diego, CA) with 5′ *Hin*dIII and 3′ *Bam*HI restriction sites. PCR amplification of pHERP was performed with a sense primer (5′-cgcgggagatctagaattcgtgagcaagggcgag-3′) that eliminates EYFP's ATG and has a *Bgl*II site (underlined) and with an antisense SP6 primer (5′-gatttaggtgacactatag-3′). The EYFP-GFPuv PCR product was subcloned downstream of ST in pcDNA3 with *Bgl*II and *Apa*I. The final construct codes for the chimeric protein with amino acids 1–70 of ST, a 3-amino acid linker (LEF) between ST and EYFP, amino acids 2–239 of EYFP, a 13-amino acid linker (GGGLEDPRVPVEK), and amino acids 1–238 of GFPuv. GT-EGFP [enhanced GFP (EGFP) targeted to Golgi with galactosyltransferase (GT)] was provided by the laboratory of Roger Tsien (Howard Hughes Medical Institute and University of California, San Diego).

In Vitro Spectra of pHERP

Bacteria expressing the various GFPs were grown overnight in liquid cultures and resuspended in one-tenth the volume of a bacterial lysis solution. Bacterial lysis solution contained (in mM) 10 Tris·HCl (pH 7.4), 100 NaCl, 1 $MgCl_2$, 10 dithiothreitol, and protease inhibitors (0.5 μg/ml aprotinin, 0.5 μg/ml leupeptin, 0.7 μg/ml pepstatin, and 20 μg/ml phenylmethylsulfonyl fluoride). Lysed bacteria were diluted into buffer containing (in mM) 50 Na-acetate, 50 glycine, and 50 K_2HPO_4, which were titrated to the various pH values with HCl or KOH. Excitation spectra were obtained with a fluorometer (Spex Flurolog 1681; Spex Industries, Edison, NJ) containing a 150-W xenon arc lamp.

Cell Culture

All cells were maintained in a 37°C incubator with 5% CO_2. All media were supplemented with penicillin, streptomycin, and glutamine. HeLa cells were maintained in DMEM supplemented with 10% FBS. JMEs (obtained from Dr. Douglas Jefferson, Tufts University) were grown in DMEM/F-12 supplemented with 10% FBS, 180 μM adenine, 5 μg/ml insulin, 5 μg /ml transferrin, 30 nM triiodothyronine, 1.1 μM hydrocortisone, 10 μg/ml EGF, and 5.5 μM epinephrine. HBE, CFT1-C2, and CFT1-CFTR cells were obtained from Dr. James Yankaskas (62) and grown in Ham's F-12 supplemented with 10 μg/ml insulin, 1 μM hydrocortisone, 25 ng/ml endothelial cell growth supplement, 10 ng/ml EGF, 30 nM triiodothyronine, 5 μg /ml transferrin, and 10 ng/ml cholera toxin.

Transfections

Cells were transiently transfected with a modified DEAE dextran protocol of Seed and Aruffo (47). Cells were sequentially split first into a tissue culture flask and, on the following day, onto glass coverslips to a confluency of ~30–50%. On the following day, the cells were incubated in a solution containing 5–6 μg/ml plasmid DNA, 100 μg/ml DEAE dextran, and 50 μM chloroquine for 2–4 h. Cells were washed with PBS containing 10% DMSO for 2 min. Medium was then added, and experiments were performed 24–72 h later. Transfection efficiency was low (1–10%) but sufficient for the single-cell experiments. Some transfections were done with a microporator. Cells plated on coverslips were exposed to DNA (2 μg/μl) while three 30-ms pulses of 300 mV/cm were applied (53). This method led to improved transfection efficiency (5–20%).

Solutions

Ringer solution contained (in mM) 141 NaCl, 2 KCl, 1.5 K_2HPO_4, 1 $MgS0_4$, 10 HEPES, 2 $CaCl_2$, and 10 glucose brought to pH 7.4 with NaOH. Na^+-free solutions contained (in mM) 141 *N*-methyl-D-glucamine (NMDG) base, 2 KCl, 1.5 K_2HPO_4, 1 $MgS0_4$, 10 HEPES, 2 $CaCl_2$, and 10 glucose brought to pH 7.4 with HCl. Calibration solutions contained (in mM) 70 NaCl, 70 KCl, 1.5 K_2HPO_4, 1 $MgS0_4$, 10 HEPES, 10 MES, 2 $CaCl_2$, and 10 glucose adjusted to various pH values (5.5, 6.0, 6.5, 7.0, 7.5, or 8.2) with KOH, 0.01 nigericin, and 0.01 monensin. In some experiments in which cells were alkalinized, NH_4Cl (30 mM) was substituted for 30 mM NaCl or NMDG where indicated. Buffer capacity experiments were performed in high-K^+/0-Na^+ solutions with varying amounts of K-acetate or NH_4Cl substituting for the KCl. Bafilomycin was used at 100–250 nM. Intracellular cAMP was increased by perfusing cells with solutions containing either 10 μM forskolin alone or 10 μM forskolin plus 500 μM dibutyryl-cAMP.

Fluorescence Ratio Imaging of pH_C and pH_G

Golgi, labeled with pHERP, and cytosol, labeled with 10 μM BCECF-AM, were monitored in separate experiments with the use of digitally processed fluorescence ratio imaging. Dye-loaded cells were placed in an open perfusion chamber on an inverted IM35 Zeiss microscope. A ×40 oil-immersion objective (1.4 NA; Nikon) was used to collect fluorescence from 1 to 30 cells during each experiment. A lens was used to focus the image through a phototube (Diagnostic Instruments) onto a low-light-level DAGE 68 SIT camera. Emission images of the cells were collected through a 530-nm bandpass filter during sequential excitation at 490 and 440 ± 5 nm (Omega Optical, Brattleboro, VT). Filters were changed with a Lambda 10-2 filter wheel (Sutter Instruments, Novato, CA). Separate images for each wavelength were averaged over eight frames by a digital image processor (Axon Image Lightning; Axon Instruments, Foster City, CA) and subsequently converted pixel by pixel to a ratio image. Data collection rate (1 ratio image every 5–60 s), filter wheel position, and shutter opening/closing were controlled by a 133-MHz Pentium computer (Gateway 2000) running the latest update of version 2.x of Imaging Workbench (Axon Instruments). The ratio images were displayed in pseudocolor.

Data were collected by electronically selecting regions of the image for quantitation. Cytosolic measurements were made from entire cells. When measurements were made on Golgi, only the brightest perinuclear regions were selected. Like FITC and BCECF, the fluorescence of pHERP excited at 490 nm increases with pH, whereas fluorescence at 440 nm is relatively insensitive to pH. Intensities were balanced with neutral density filters. Photobleaching was negligible during our experiments.

Methods describing calibration of cytosolic and organelle pH measurements have been reported previously (54).

Determination of Golgi Buffer Capacity

We made small, stepwise changes in the extracellular concentration of either NH_4^+ or acetate (OAc^-) in the absence of extracellular Na^+ to induce defined changes in pH_G, which were then used to calculate Golgi buffer capacity (β_G) over a range of pH values. Using measured pH_G values and assuming that the Golgi concentration of the uncharged species equaled the external concentration, we calculated [NH_4^+] or [OAc^-] using the Henderson-Hasselbalch equation ($K_a = 5.6 \times 10^{-10}$ for the weak base reaction and 1.8×10^{-5} for the weak acid reaction, where K_a is the equilibrium constant). Golgi buffer capacity was then calculated for the midpoint of the pH change (ΔpH) according to the following equation (41)

$$\beta_G = \frac{-[NH^{4+}]_G}{\Delta pH} \qquad \beta_G = \frac{[OAc^-]_G}{\Delta pH} \tag{1}$$

Calculation of H^+ Permeability of Golgi Membranes

We used the previously described model (18), which accurately describes experimentally determined values of both steady-state and transient acidification of endosomes (56) and Golgi (61), and experimentally determined changes of pH_G, pH_C (measured in separate but identical experiments), and β_G to calculate P_{H^+} of the Golgi. The model assumes that changes in pH_G result from a competition between V-ATPase-mediated H^+ pumping and passive H^+ leak (which is characterized by P_{H^+}) out of the Golgi into the cytosol. It should be noted that the predicted values of active pump numbers and P_{H^+} did not drastically change when the complicated molecular model of the V-ATPase was replaced by a simpler model in which the H^+ flux was proportional to the proton motive force working against the pump (18). Thus our calculations of P_{H^+} were insensitive to the specific molecular model of the H^+ pump.

One experimental protocol was to add the H^+ V-ATPase inhibitor bafilomycin to cells and model measured rates of alkalization of pH_G while pH_C remained constant (see Fig. 8*A*). The second approach was to acidify both cytosol and Golgi cells with an NH_4Cl pulse and then to model changes of pH_G while pH_C also changed (see Figs. 6 and 8*B*). Without loss of generality, the equation that describes transient changes in pH_G during the above-mentioned experimental manipulations is

$$\frac{dpH}{dt} = \frac{1}{\beta_G} \cdot \frac{S}{V} \cdot (J_{leak} - \rho_{pump} \cdot J_{pump}) \tag{2}$$

where J_{pump} is the H^+ flux of an individual V-ATPase, ρ_{pump} is the density of H^+ pumps in the Golgi, and J_{leak} is the passive flux of H^+ across a unit area of Golgi membrane; the term in parentheses is the total flux of H^+ across a unit area of membrane. These fluxes depend on the Golgi-cytosol [H^+] gradient, the change in pH defined as $pH_G - pH_C$, and the membrane potential (Ψ_G). *S* and V are the Golgi surface area and volume, which were assumed to be 8×10^{-6} cm^2 and 6×10^{-12} cm^3, respectively (30). β_G is the buffering capacity of the Golgi (determined as in Fig. 7).

Using the previously described model of the V-ATPase (19), we found computed values for J_{pump} to be relatively constant over moderate luminal pH ranges but sensitive to changes in membrane potential (calculated as shown in *Eq. 4*), consistent with previous current-voltage data (7). In the present work, calculated J_{pump} changed by only 1–10% over the time course of any experiment.

Although the true nature of the proton leak, J_{leak}, is not known, we modeled this transport as simple, passive diffusion (23)

$$J_i = P_i \cdot \frac{z_i \cdot U \cdot ([C_i]_G - [C_i]_C \cdot e^{-z_i U})}{1 - e^{-z_i U}} \quad (3)$$

where i denotes the ionic species, J_i is the ionic flux density, P_i is the permeability of the membrane to ion i, $[C_i]_C$ and $[C_i]_G$ are the concentrations of the ion in the cytoplasm and Golgi, respectively, z_i is the valance of the ion, and $U = \Psi_G F/(RT)$, where U is reduced voltage, Ψ_G is the Golgi membrane potential, and F, R, and T have their usual meanings.

Because Ψ_G will affect both J_{pump} and J_{leak}, we included this effect by writing an explicit form for Ψ_G in terms of the excess charge inside the Golgi, the membrane of which was treated as a parallel plate capacitor, and by assuming that the dominant counterions were K^+ and Cl^-

$$\Psi_G = \frac{F \cdot V}{C_m} \cdot ([K^+]_G - [Cl^-]_G + \int_{pH_C}^{pH_G} \beta_G \cdot dpH - B) \quad (4)$$

where C_m is the total capacitance of the membrane, $[K^+]_G$ and $[Cl^-]_G$ are the molar concentrations of K^+ and Cl^- in the Golgi, the integral term represents the total amount of H^+ in the Golgi lumen (buffered plus free), and B (a constant) is the molar concentration of charged species that are trapped in the Golgi. When the concentration of trapped protein, B, is balanced by the net sum of all ionic species in the lumen, Ψ_G is zero.

When K^+ and Cl^- permeabilities were assumed to be 10^{-5} cm/s (22), Ψ_G was calculated (from *Eqs. 2* and *3*) to be <10 mV. This result was consistent with recent experiments showing that the Golgi and *trans*-Golgi network had relatively large conductances to both K^+ and Cl^- and that Ψ_G was likely to be an unimportant determinant of either J_{pump} or J_{leak} (43, 61). Schapiro and Grinstein (43) arrived at this conclusion by finding that $[K^+]_G$, measured to be 107 mM using a null point method, was similar to the cytosolic $[K^+]$ ($[K^+]_C$).

Equation 2 together with equations describing the passive fluxes of K^+ and Cl^- (from *Eq. 3*) forms a set of three ordinary differential equations that are coupled by the algebraic constraint of *Eq. 4* and that uniquely determine the time course of changes of ionic concentrations in the Golgi given an initial set of conditions. We assumed $[K^+]_C$ = 130 mM and $[Cl^-]_C$ = 20 mM throughout each experimental run, and initial $[K^+]_G$ and $[Cl^-]_G$ were chosen to keep the Golgi close to electroneutral (consistent with $\Psi_G < 10$ mV).

pH_C and transient changes of pH_G (similar to those shown in Fig. 8, *A* or *B*) were measured in separate experiments, and then the model was used (*Eq. 3*) to predict the changes in Golgi acidification. This was done by varying P_{H^+}, ρ_{pump}, and the concentration of fixed negative charge in the lumen (B) until a best fit to pH_G was obtained. When results were modeled from experiments using V-ATPase inhibitors (similar to Fig. 8*A*), ρ_{pump} was set to zero and pH_C was held constant to match experimental conditions. The Na^+-free, acid-loaded Golgi experiments (see Fig. 8*B*) were more complex because pH_C and pH_G both varied. However, this procedure was advantageous because it allowed us to acidify the Golgi and keep pH_C relatively constant (see Figs. 6 and 8*B*). For these experiments, we reported the average of six predicted P_{H^+} values, for each pH_G experiment, where each pH_G run was fit against a different pH_C run (see *Possible errors in predicting P_{H^+}*). All searches were performed with a Nelder-Mead algorithm, and the ordinary differential equations were solved with a stiff method in both Matlab and Berkeley Madonna software (38).

Although *Eqs. 2–4* yielded estimates of P_{H^+}, B, and the number of active H^+ V-ATPases (NOP = $\rho_{pump} \cdot S$), we have reported only predicted values for P_{H^+}. The model yielded average values of $B \approx 140$ mM and NOP $\approx$ 2,000. Within a particular data set, these two parameters had counteracting effects: a decrease in ρ_{pump} together with an increase in B sometimes resulted in very similar pH fits. This made it very difficult for the search algorithm to find a unique, best fit, and the same data set with different initial search conditions would yield very different values for B and ρ_{pump}. In contrast, estimates of P_{H^+} were more robust to the initial conditions of the search algorithm, and the same best value for P_{H^+} was usually found regardless of the values of B and ρ_{pump}. As mentioned above, J_{pump} changed little for any given run. Thus the parameter P_{H^+} had the strongest influence over the shape of the predicted pH curves.

It should be noted that in the limit of Ψ = 0 mV, *Eqs. 2–4* can be replaced by an intuitive and simple expression for the P_{H^+} of the Golgi in terms of the instantaneous rate of change of the Golgi, the H^+ gradient, and a few physical parameters

$$\frac{dpH_G}{dt} = \frac{1}{\beta_G} \cdot \frac{S}{V} \cdot P_{H^+} \cdot ([H^+]_G - [H^+]_C)$$
$$\Rightarrow P_{H^+} = \frac{dpH_G}{dt} \cdot \frac{V}{S} \cdot \frac{\beta_G}{([H^+]_G - [H^+]_C)} \quad (5)$$

Thus P_{H^+} could also be determined from initial rates of alkalinization after treatment with bafilomycin to block the H^+ pumps without appealing to the more complicated model. For the bafilomycin-treated Golgi, this method predicted P_{H^+} values that were within factors of 2–4 of the values determined using the full model.

Possible Errors in Predicting P_{H^+}

There are several uncertain parameters and assumptions that affect our estimates of P_{H^+}. We explored how errors in each of the following affected the predicted value of P_{H^+}.

Surface-to-volume ratio. We arbitrarily chose the value of 1.33×10^{-6} cm^{-1} for the surface-to-volume ratio (S/V) of the Golgi obtained from rat kidney cells (30). Golgi S/V in terminal tubule and acinar cells of the rat submandibular gland (51) is an order of magnitude smaller. If the latter estimates were correct, our P_{H^+} values would be 10-fold larger; thus our calculations provide a lower estimate. This S/V parameter is most likely the largest source of error in our study.

Buffering. If the true buffering capacity is 20% larger or smaller than the value measured, which is consistent with our errors, then the true P_{H^+} will be 20% larger or smaller than predicted.

H^+ gradients. In many of the bafilomycin-induced alkalization experiments, pH_C was assumed to be 7.55 (the average value). Varying the assumed pH_C by ±0.2 pH units for a typical run had a ±25% effect on the estimated P_{H^+}. For the experiments where the Golgi has been acidified, each pH_G run (see examples in Figs. 6 and 8*B*) was fit against six pH_C

runs that represented the entire set of measured cytoplasmic recovery experiments. Most of these reported P_{H^+} values had SD of 2×10^{-4}, although one had a SD of 2×10^{-3}.

Membrane potential. The movement of counterions influences H^+ movement through effects on Ψ_G as shown in *Eq. 4*. When the Golgi membrane was assumed to have K^+ and Cl^- permeabilities $>5 \times 10^{-9}$ cm/s, Ψ_G was calculated (from *Eqs. 2* and *3*) to be <10 mV. When permeabilities to K^+ and Cl^- were $<5 \times 10^{-9}$ cm/s, K^+ and Cl^- movements became quite slow, and Ψ_G began to affect pH_G. The present P_{H^+} predictions remain unchanged for K^+ and Cl^- permeabilities $>5 \times 10^{-9}$ cm/s. Below this value, movements of counterions resulted in transient changes of Ψ_G that affected calculations of P_{H^+}. When Ψ_G was arbitrarily varied from +7 mV to +50 mV and held constant over the time course of the simulation, the predicted P_{H^+} values varied from +50% to −50% of the original value determined with our model of Ψ_G. Therefore, the P_{H^+} values determined with *Eqs. 2* and *3* were relatively insensitive to Ψ_G.

Obtaining Initial Alkalization Rates and P_{H^+} From the Literature

To compare our data with those from previous work, we scanned published figures as PICT files and used Data Thief (Computer Systems Group of the Nuclear Physics Section at the National Institute for Nuclear Physics and High Energy Physics, Amsterdam, The Netherlands) to extract data points of pH_G vs. time. These data points were then used to obtain initial rates or were used with the model (*Eqs. 2–4*) to determine P_{H^+} (see Table 2).

Statistics

Unless otherwise specified, data have been presented as means ± SD. Experimental data were compared using unpaired Student's *t*-test (two-tailed). Differences were considered significant if $P < 0.01$.

As an objective measure of the quality of our fits, the conventional root mean square (RMS) value was computed. When a particular run did not have an RMS value <0.175 pH units, it was dropped from the analysis. The average RMS value for all runs fit by the model was 0.06 ± 0.03 pH units (mean ± SD).

RESULTS

pH Sensitivity and Golgi Targeting of pHERP

The ST-containing compartment was targeted with pHERP. We first created a chimeric protein of two commercially available mutant GFPs by placing GFPuv NH_2-terminal to EYFP. The chimeric protein retains the dominant excitation peaks of the individual molecules at 397 nm (GFPuv) and ~500 nm (EYFP) when emission intensity is measured at 520 nm (Fig. 1). The peak at 500 nm was extremely sensitive to pH, whereas the trough at ~440 nm was relatively insensitive to pH, indicating that this molecule could be used as an excitation ratiometric (490/440) pH indicator. By leaving the luminal and transmembrane amino acids (1–70) of ST intact and replacing its cytosolic domain with pHERP, we were able to target the pH sensor to the Golgi lumen (Figs. 1 and 2). ST was used to target pHERP because it is one of the *trans*-Golgi enzymes (52) whose activity has been proposed to be altered in CF (2). Cells transiently expressing ST-pHERP displayed the characteristic perinuclear staining pattern typical of Golgi. A typical result for JME cells is shown in Fig. 2, and similar staining patterns were observed in HeLa, HBE, CFT1, and CFT1-CFTR cells (not shown). An in vivo calibration was performed at the end of every experiment (Fig. 1) by perfusing solutions containing nigercin (K^+/H^+ exchanger) and monensin (Na^+/H^+ exchanger) with different pH values onto the cells. The pK_a of the ratio 490/440 was ~6.5 and thus was optimal for measuring pH_G (Fig. 1).

pH_G Measured With pHERP

We performed control experiments on HeLa cells to compare measurements of pH_G obtained using ST-pHERP with previous measurements of HeLa cell pH_G obtained using other methods. As shown in the typical individual experiment and in the summarized data (Fig. 3), steady-state pH_G was 6.4, in good agreement with previous results of 6.4–6.6 obtained using Golgi-targeted fluorescein and GFP-based pH sensors (26, 32, 61). When HeLa cells were pulsed with a solution containing 30 mM NH_4Cl, pH_G instantly alkalinized because of the entry of the weak base NH_3. With removal of the NH_4Cl, the cells acidified below basal levels and rapidly recovered (Fig. 3). These results were in good agreement with results obtained in Vero cells using FITC-verotoxin (27, 43) and in CHO cells using a mutant GFP (28).

ST-pHERP consists of ST fused to the relatively pH-insensitive GFPuv and pH-sensitive EYFP. EYFP has recently been reported also to be sensitive to $[Cl^-]$, with decreases in $[Cl^-]$ causing increases in fluorescence (57). Although the changes in EYFP fluorescence due to changes in $[Cl^-]$ are smaller than those due to pH (32, 57), we were concerned that changes in ST-pHERP fluorescence ratio in vivo would be larger than predicted from calibrations in which pH was varied but $[Cl^-]$ was held constant. We therefore compared measurements of pH_G made with ST-pHERP with those obtained with GT-EGFP (13, 28, 32). EGFP is insensitive to $[Cl^-]$ but sensitive to pH, with a pK_a of 6.4 (32, 57). When expressed in both CFT1 and CFT1-CFTR cells, GT-EGFP and ST-pHERP yielded similar results when pH_G was perturbed. When cells expressing either ST-pHERP (see Fig. 6) or GT-EGFP (data not shown) cells were pulsed with NH_4Cl followed by removal and then Na^+-free treatment, pH_G acidified and recovered partially. Full recovery was completed only when Na^+ was added back to the cells. These results support the conclusion that ST-pHERP was accurately reporting pH_G. The fact that ST-pHERP was more easily calibrated in terms of pH_G made it preferable to GT-EGFP.

CFTR and Steady-State pH_G

As summarized in Table 1, pH_G in respiratory epithelial cells was more alkaline (6.7–7.0) than in HeLa cells (6.4; see Fig. 3). Airway epithelial cells from ΔF508-CF patients (CFT1 and JME) had pH_G values of

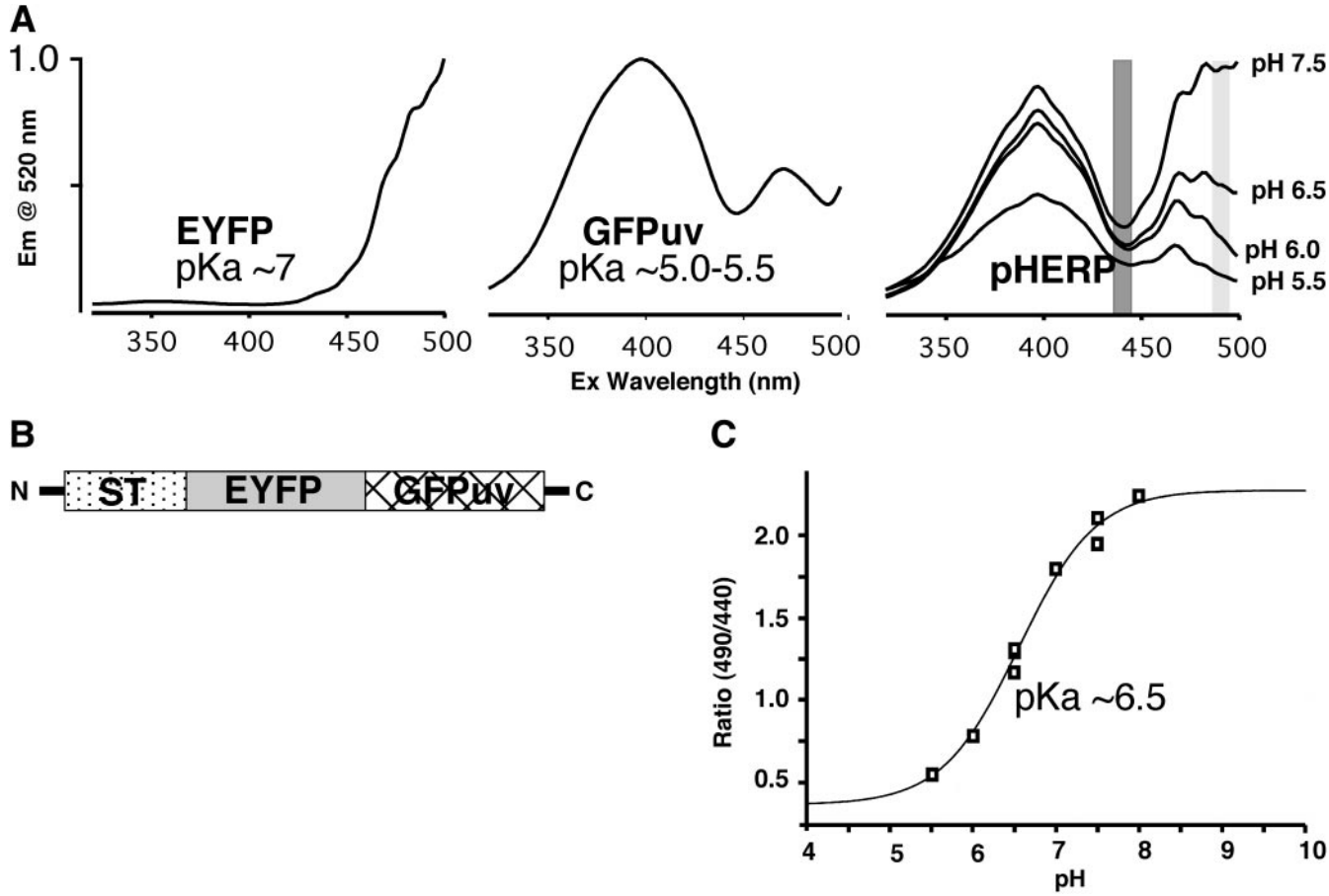

Fig. 1. Construction of sialyltransferase (ST)-pH-sensitive excitation ratiometric green fluorescent protein (pHERP). *A*: in vitro excitation spectrum of green fluorescent protein (GFP) constructs measured at 520 nm. Spectra for enhanced yellow fluorescent protein (EYFP) and ultraviolet enhanced GFP (GFPuv) were obtained at pH 7.5. EYFP and GFPuv were fused together, separated by a 13-amino acid linker to create pHERP. The spectrum of pHERP is extremely sensitive to pH at ~490 nm and relatively insensitive at 440 nm, allowing for ratiometric imaging (ex, excitation). *B*: schematic of ST-pHERP. Amino acids 1–70 of ST were used to target pHERP to the Golgi. N, NH_2 terminal; C, COOH terminal. *C*: representative in vivo calibration of ST-pHERP (performed at the end of each experiment). Golgi pH was allowed to equilibrate with solutions of various pH values in the presence of 10 μM each of nigericin and monensin.

6.7 and 7.0, respectively, while those from WT-CFTR cells (CFT1-CFTR and HBE) had pH_G values of 6.9 and 6.7, respectively. When the genetically matched CFT1 cells were compared with CFT1-CFTR cells, the ΔF508-expressing CFT1 cells were 0.2 pH units more acidic ($P < 0.01$). There was no significant difference in pH_C (7.4–7.6) among the various cells.

The activity of CFTR is increased by cellular cAMP concentration, and the effects of cAMP on pH_G have been controversial (32, 48). We therefore tested the effects of cAMP in CFT1 and CFT1-CFTR cells. In both cell types, there was little change in pH_G in response to cAMP whether experiments were performed in the presence of 25 mM HCO_3^-/5% CO_2 or in nominally HCO_3^--free solutions (Fig. 4).

Golgi H^+ "Leak" and Potential Effect of CFTR

We determined the role of CFTR in controlling H^+ leak across the Golgi membrane into the cytosol in CFT1 and CFT1-CFTR cells that had been treated with bafilomycin. Once the bafilomycin effect had reached a steady state with pH_G and pH_C approximately equal, cells were treated with an NH_4Cl pulse followed by the Na^+-free condition. This caused both the Golgi and the cytosol to acidify. We then added back extracellular Na^+, which allowed both pH_G and pH_C to realkalinize. Rates of alkalinization of the Golgi lumen (using ST-pHERP) and cytosol (using BCECF) were measured in separate experiments. It was expected that if the H^+ leak in the Golgi were large, removal of H^+ from the cytosol by the Na^+/H^+ exchanger (NHE) in the plasma membrane would cause a similarly rapid alkalinization of pH_G because H^+ in the Golgi lumen would rapidly leak into the cytosol to be pumped out of the cell across the plasma membrane by the NHE. By comparing recovery rates of pH_C and pH_G measured using the same experimental protocol, we found that the Golgi in CFT1 cells alkalinized at a rate of 2.2 ±

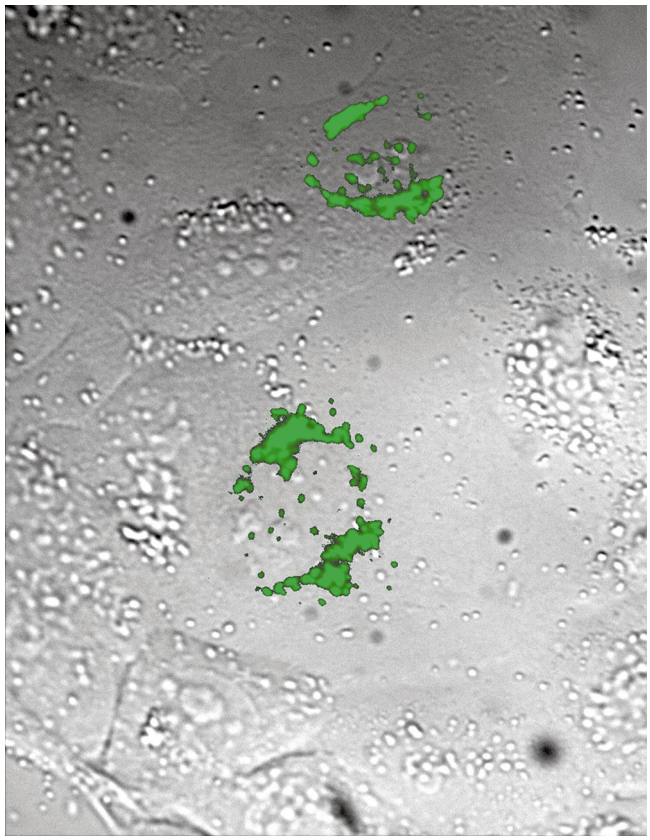

Fig. 2. ST-pHERP morphology. Human nasal epithelial (JME) cells were transiently transfected with ST-pHERP and mounted on the stage of the microscope. Fluorescence image overlaid on the bright-field image shows that pHERP exhibit a perinuclear staining pattern typical of Golgi.

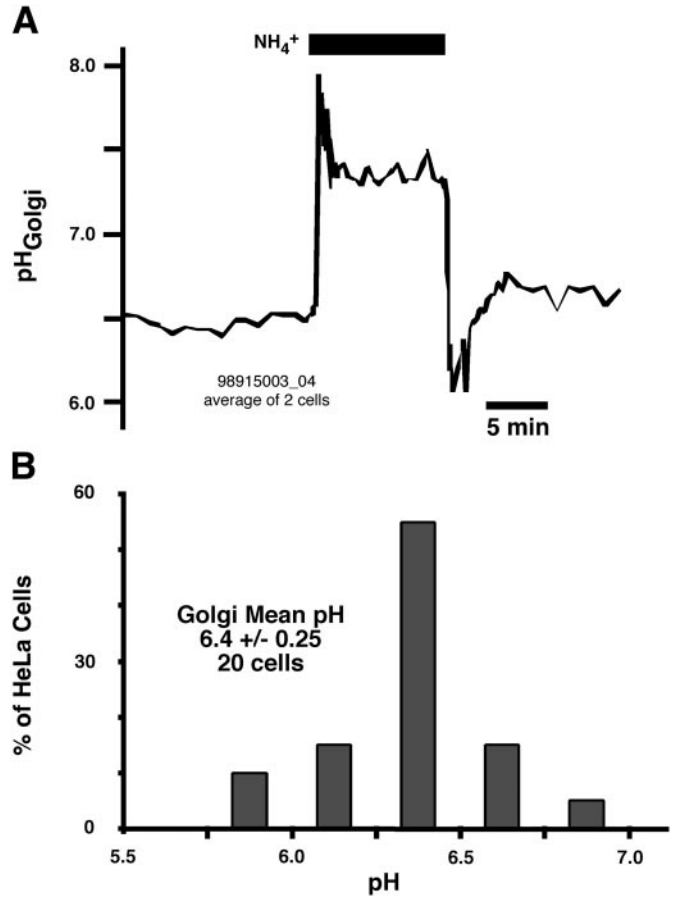

Fig. 3. ST-pHERP reports Golgi pH (pH_G) in HeLa cells. *A*: a pulse of 30 mM NH_4Cl alkalinized the Golgi due to NH_3 entry. The slower NH_4^+ entry led to a slight acidification, which was apparent when the NH_4Cl was washed away. Golgi pH rapidly recovered from the acidification. *B*: histogram of steady-state pH_G measured with ST-pHERP at the beginning of each experiment.

0.7×10^{-2} pH units/s ($n = 9$), while the cytosol alkalinized at a rate of $5.0 \pm 1.6 \times 10^{-2}$ pH units/s ($n = 33$). Experiments on CFT1-CFTR cells showed that pH_G and pH_C alkalinized at rates similar to those in CFT1 cells. These data implied that the Golgi membrane had a large P_{H^+} that was unaffected by the presence or absence of CFTR.

Golgi-to-Cytosol [H^+] Gradient

We compared pH_C and pH_G from experiments in which the CFT1 cells were acidified with a 5-min pulse of 30 mM NH_4^+ followed by Na^+-free Ringer. Removal of extracellular Na^+ prevented the NHE in the plasma membrane from pumping out the accumulated H^+. On average, the steady-state pH_C of CFT1 cells was 7.5 ± 0.2 ($n = 68$), while under the conditions used to acidify the cells, pH_C dropped to 6.4 ± 0.2 ($n = 55$). Under the same conditions, average pH_G dropped from 6.7 ± 0.2 ($n = 45$) to 5.9 ± 0.3 ($n = 31$) and then partially recovered with a single-exponential time course (see Fig. 6*C*). The average [H^+] gradient (Golgi to cytosol) returned to 2×10^{-7}, close to the value exhibited under control conditions (1.7×10^{-7}) after ~7 min (Fig. 6).

Golgi H^+ Permeability and Buffer Capacity

When the H^+ V-ATPase was inhibited by bafilomycin, the Golgi rapidly alkalinized with an initial rate of $8.6 \pm 7.8 \times 10^{-3}$ pH units/s ($n = 9$; Fig. 5). This result was similar to those in previously published experi-

Table 1. *Steady-state pH_G and pH_C*

	Golgi pH	Cytosol pH	ΔpH (Δ[H^+])
HeLa	6.4 ± 0.3 (20)	7.4 ± 0.2 (110)	1 (3.6×10^{-7})
CFT1	6.7 ± 0.2 (45)	7.5 ± 0.2 (68)	0.8 (1.7×10^{-7})
CFT1-CFTR	6.9 ± 0.3 (29)	7.6 ± 0.2 (91)	0.7 (1×10^{-7})
JME	7.0 ± 0.2 (26)	7.6 ± 0.3 (246)	0.6 (0.75×10^{-7})
HBE	6.7 ± 0.2 (13)	ND	ND

Values for Golgi pH (pH_G) and cytosol pH (pH_C) are means ± SE; numbers in parentheses indicate number of cells. pH_G and pH_C were measured in HeLa, cystic fibrosis tracheal (CFT1), cystic fibrosis transmembrane conductance regulator (CFTR)-expressing CFT1 (CFT1-CFTR), human nasal epithelial (JME), and human bronchial epithelial (HBE) cells during incubation of the cells in control Ringer. The change in pH (ΔpH) represents the Golgi-to-cytosol pH gradient, whereas Δ[H^+] represents the Golgi-to-cytosol proton concentration gradient. ND, not determined.

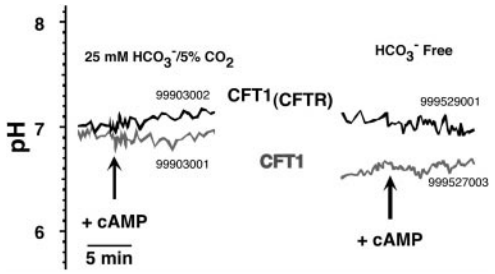

Fig. 4. Increasing cAMP concentration does not alter pH_G. *Left*: experiments were conducted in the presence of 5% CO_2 and 25 mM HCO_3^-. Intracellular cAMP concentration was increased by application of 10 μM forskolin (arrow). *Right*: experiments were conducted in HEPES-buffered nominally HCO_3^--free conditions. cAMP concentration was increased by application of 10 μM forskolin and 500 μM dibutyryl-cAMP (arrow). Traces are from Golgi of single cells. CFTR, cystic fibrosis transmembrane conductance regulator; $CFT1_{(CFTR)}$, CFTR-expressing tracheal cells.

ments (summarized in Table 2) on HeLa, Vero, and CHO cells obtained by using a variety of methods and indicated that the Golgi had a large H^+ leak that ordinarily counters the H^+ pump (13, 26, 32, 42, 43, 61). These observations led to the qualitative conclusion that P_{H^+} was large. Data from these experiments can also be used to calculate P_{H^+}, but the Golgi buffer capacity must be known.

It is well established that the cytosolic buffering capacity varies with pH (58, 59), which is a function of the pK_a and concentration of titratable groups (41). Previous measurements of Golgi buffer capacity have reported only one value (42, 61) or claimed that β_G was constant between pH 6 and 7 (13). We felt that it was necessary to measure β_G over a wide pH range to calculate P_{H^+} of the Golgi at the various pH values observed in our experiments. Values for β_G were obtained by first treating the cells with bafilomycin (250 nM) and then titrating in various amounts of weak base (NH_3) or weak acid (HOAc). We measured β_G at pH < 7 by following the bafilomycin treatment with an acidification step (NH_4Cl prepulse followed by incubation in Na^+-free solution) and then adding either NH_4Cl or HOAc to the Na^+-free solutions. A typical experiment in which β_G was measured is shown in Fig. 7*A*. Data summarizing measurements of β_G as a function of pH are summarized in Fig. 7*B*. Buffer capacities were grouped into 0.2-pH unit buffering domains for simplicity. At pH 6.9 ± 0.02 (mean ± SE), $\beta_G = 17.2 \pm 4$ mM per pH unit (mean ± SE), in good agreement with previous results of 10–40 mM per pH unit (13, 42, 61). At higher and lower pH values, β_G varied, and the variation was well fit by a single exponential (Fig. 7*B*), which allowed us to extrapolate to acidic values that were attained in some measurements of P_{H^+}.

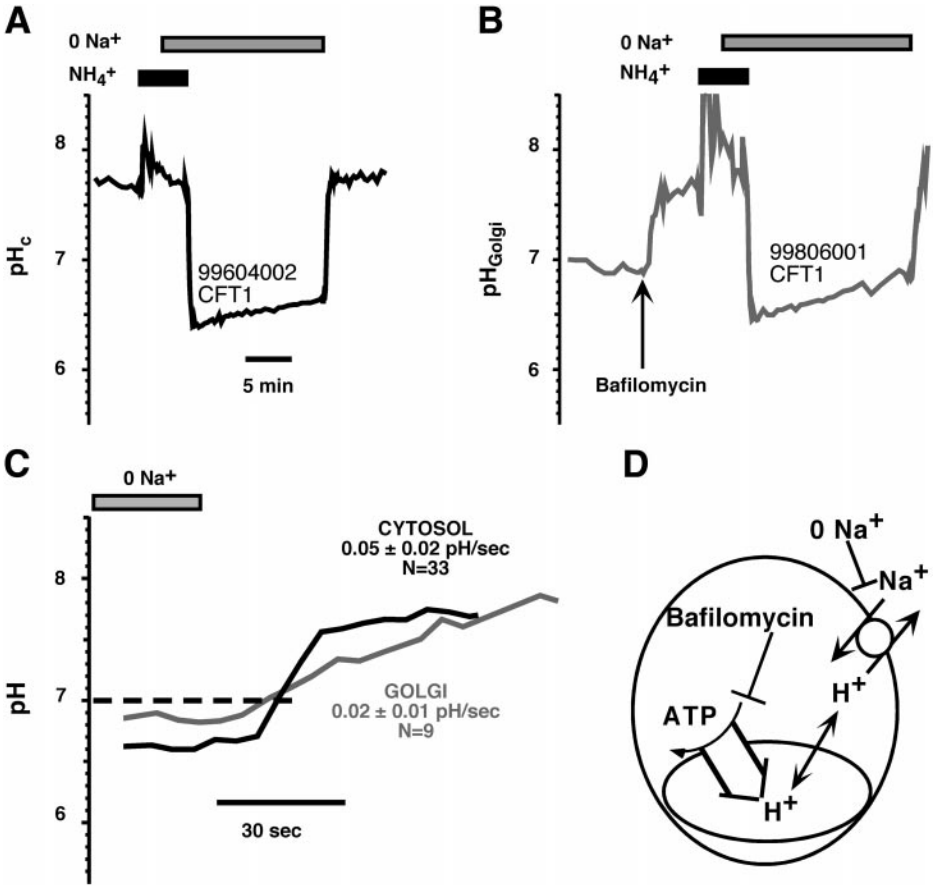

Fig. 5. The Golgi H^+ leak is large. *A*: a representative trace of cytosolic pH (pH_C). Cells were exposed to a pulse of 30 mM NH_4Cl for 5 min, and Na^+ was then replaced with *N*-methyl-D-glucamine (NMDG) 2.5 min into the NH_4Cl pulse. When NH_4^+ was removed, the cells acidified and remained acidic. Reapplication of Na^+ allowed pH_C to recover to control levels. *B*: a representative trace of pH_G during an experiment similar to that performed on the cytosol in *A*, although the cell was first exposed to bafilomycin (250 nM), a specific inhibitor of the H^+-ATPase. *C*: cytosolic and Golgi pH alkalization curves from *A* and *B* are superimposed and the time scale is magnified. Slope at pH 7 was taken for a number of similar experiments. *D*: model of the likely transporters and channels that are regulating pH during the experiment.

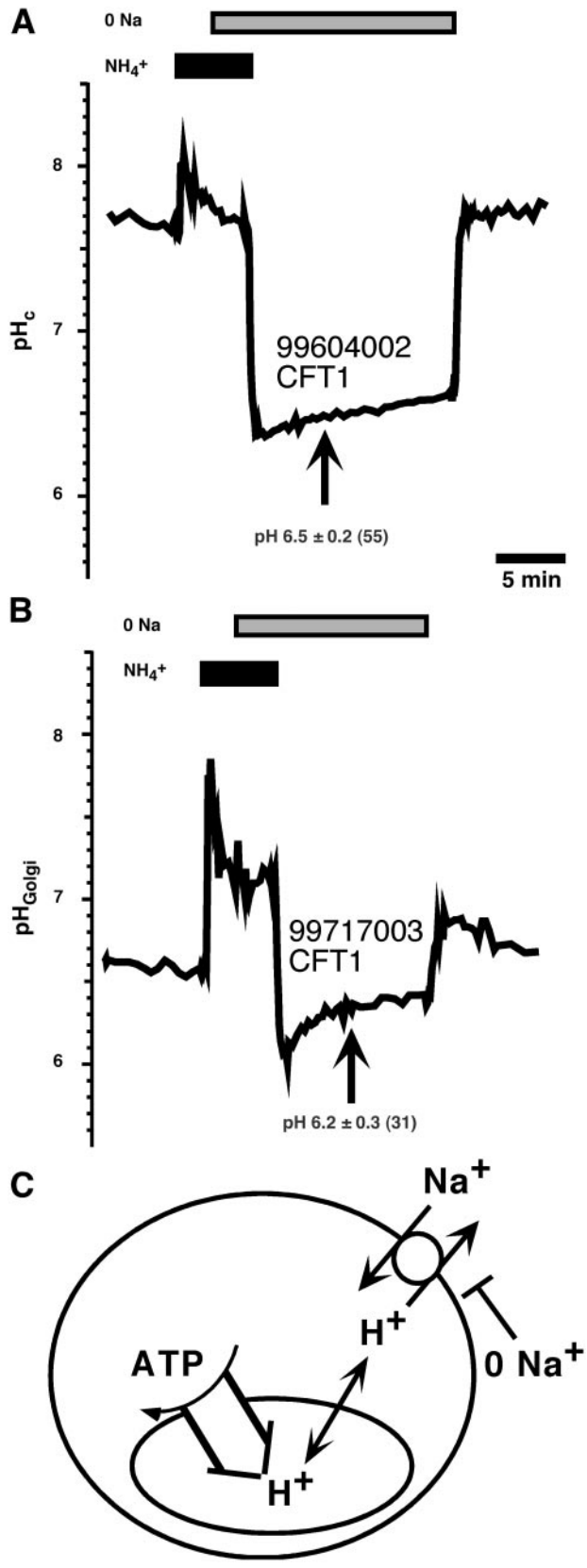

Fig. 6. Golgi recovery from an acid load is partially dependent on extracellular Na^+. *A*: the same representative pH_C trace from Fig. 5. *B*: representative trace of pH_G during the same protocol performed on the cell in *A*. *C*: model of the likely transporter and channels regulating pH during the experiment.

By using the experimentally determined β_G and a model of pH_G (*Eqs. 2–4*), we were able to estimate the P_{H^+} of bafilomycin-treated cells when pH > 6.4 (Fig. 8, *A* and *C*). Additionally, the model allowed estimates of P_{H^+} under various conditions where organelle and pH_C varied over a considerable range: recovery of both pH_G and pH_C were measured after acidification (using an NH_4^+ prepulse) and treatment with Na^+-free solution (see example in Fig. 8, *B* and *C*). These data provided P_{H^+} when $pH_G < 6.4$. These calculations showed that the log of Golgi P_{H^+} was inversely correlated with the pH_G (Fig. 8*C*). The data were well fit by a linear equation, and the slope of this line was significantly different from the slope of 0 ($P < <0.01$).

DISCUSSION

ST-pHERP for Measuring pH_G

By fusing EYFP and GFPuv, each having different excitation spectra and different pH dependencies, we created the genetically targeted ratiometric pH indicator pHERP (Figs. 1 and 2). A variety of other techniques have been used to measure pH_G, but each has limitations that our technique attempted to improve. Isolated Golgi vesicles are rarely pure and can be damaged and lose soluble regulatory factors during preparation. Electron microscopic methods (2) allow only imprecise quantitation at single time points. Microinjection of dye-filled liposomes (48, 49) is laborious and invasive, and since the dyes are delivered to the Golgi relatively slowly and then removed relatively rapidly at 37°C, measurements can be performed only during short time periods. FITC-labeled β-subunits of toxins (27, 42–44) can be used only in cells that express the toxin receptors. Genetic targeting of "receptors" and then adding membrane-permeant, pH-sensitive, fluorescent "ligands" to label the receptors (13, 61) requires complicated chemical syntheses and loading procedures.

GFPs have many advantages as organelle pH sensors: any organelle can be targeted, a variety of mutants with a wide range of pK_a values (5.5–7.0) is available (28, 32, 55), and changes of pH can be measured with little background signal, no diffusive loss of fluorophore, minimal bleaching, and no requirement for exogenous dyes that require hydrolysis and might lead to cytotoxicity. Despite these many advantages, calibrating the single-wavelength intensity changes of these GFPs is problematic, because artifacts can arise when apparent fluorophore concentration changes and pH does not. Miesenbock et al. (34) overcame this problem by developing a GFP with a spectrum that shifted with pH, thereby providing an excitation ratiometric pH indicator. Our development of pHERP al-

Table 2. *Summary of Golgi P_{H^+}*

	pH_G	pH_C	Initial slope, pH U/s	P_{H^+}, cm/s	References
CFT1	6.6 ± 0.33 ($n = 12$)	7.5	$8.6 \pm 6.7 \times 10^{-3}$ ($n = 12$)	$0.54–3.3 \times 10^{-3}$	Present study
CFT1-CFTR	6.7 ± 0.34 ($n = 6$)	7.6	$10 \pm 5.6 \times 10^{-3}$ ($n = 6$)	$1–2.5 \times 10^{-3}$	Present study
HeLa	6.5		8.7×10^{-3}	5.7×10^{-4} (*a*)	*32,* Fig. 5*A*
Vero	6.5	7.2	2.5×10^{-3}	5.8×10^{-4} (*b*)	*43,* Fig. 5*A*
	6.6		3.4×10^{-3}	3.9×10^{-4} (*c*)	*27,* Fig. 10*A*
CHO	6.4	7.4	4.3×10^{-3}	9.3×10^{-4} (*d*)	*13,* Fig. 3*B*

Values for pH_G (rounded to the nearest 10th of a pH unit) are from the specific traces used to obtain the tabulated proton membrane permeability (P_{H^+}) values; values for pH_C are average values published for the indicated cell types. Values for initial slope represent initial alkalinization rates (obtained from referenced articles as described in METHODS) measured just after the V-ATPase had been inhibited with either bafilomycin or concanamycin (assuming drugs acted instantly). P_{H^+} was calculated from *Eqs. 2–4* and buffer capacity measured in Fig. 8*B; a–d* refer to points inserted into Fig. 8*B*. Figures cited are published in the referenced article from which data were obtained.

lows an alternative approach that has many of the same advantages as pHlorin for measuring pH_G.

CFTR, Counterion Conductance, and Membrane Potential in Determining pH_G

As measured with pHERP, HeLa cells had an average pH_G of 6.4 (Fig. 3), which was nearly identical to previous measurements obtained using a variety of other methods in HeLa, fibroblast, and Vero cells (27, 32, 42, 43, 61). In contrast, the Golgi of airway epithelial cells was more alkaline (pH_G = 6.7–7.0) than in HeLa cells. Although, there was no clear correlation between the presence of CFTR and pH_G when all the airway epithelial cells were compared, there was a significant difference when the genetically matched CFT1 cells were compared (Table 1). Cells expressing ΔF508-CFTR had a pH_G of 6.7 (CFT1) and 7.0 (JME), while those expressing WT-CFTR had a pH_G of 6.9 (CFT1-CFTR) and 6.7 (HBE). The finding that ΔF508-CFTR-expressing CFT1 cells were more acidic (0.2 pH units) than the WT-CFTR-expressing CFT1-CFTR cells is a result directly opposite the trend measured by Barasch et al. (2). The pH dependence of ST can be quite variable depending on the particular isoform and cell type involved (3, 4, 16, 36), so the potential significance of this small difference in Golgi acidity in CF remains to be determined. It seems likely that the results of Barasch et al. (2) were influenced by the technical problems associated with isolating purified Golgi and the relative insensitivity of the electron microscopic dinitrophenol-3-(2,4-dinitroanilino)-3′-amino-*N*-methyldipropylamine (DAMP) method. Our data (also see Refs. 12 and 49) therefore showed that the chronic lung infection of CF is not due to an alkaline pH_G. Indeed, the presence of CFTR in CFT1 cells was correlated with significant alkalinization, not acidification, of pH_G.

Al-Awqati and colleagues (1, 2) suggested that the Golgi Cl^- permeability was able to limit H^+ flux by dissipating the membrane potential. Subsequent data in the literature indicated that conductances to both K^+ and Cl^- in the Golgi and *trans*-Golgi network are so high that membrane voltage is small and unimportant in determining organelle pH (10, 43, 61). This is consistent with observations that neither ouabain nor its membrane-permeant analog acetyltrophanthidin have any effect on pH_G in HeLa cells, which have no CFTR (Wu M and Machen T, unpublished observations), implying that the Na^+-K^+-ATPase activity was low or nonexistent. Our model confirmed and extended the conclusions regarding the small Golgi membrane potential and also allowed us to estimate the number of counterion channels necessary to achieve this goal. Our model showed that K^+ and Cl^- permeability could be decreased to as low as 5×10^{-9} cm/s before membrane potential became a factor in fitting the pH transients (see METHODS and Fig. 8). For a Golgi with a surface area of 8×10^{-6} cm^2 (30), these very low permeabilities corresponded to K^+ and Cl^- conductances <20 pS for the entire Golgi, which could be achieved with between one and two K^+ or Cl^- channels. Calculation of K^+ conductance was performed by using the Goldman-Hodgkin-Katz (GHK) current equation (23) after compensating for the assumed surface area of the Golgi. Conductance was calculated as the slope of the current with respect to voltage at 0 mV, assuming $[K^+]_G$ = 110 mM (43) and $[K^+]_C$ =130 mM. In this circumstance, it is likely that eliminating CFTR has no effect on pH_G, because other K^+ and Cl^- channels can provide sufficient counterion conductance to ensure that membrane potential in the Golgi is small and therefore has little effect on H^+ pumps or leaks. Two other studies have provided evidence for the presence of Cl^- channels in the Golgi: Nordeen et al. (35) found an anion channel in enriched Golgi fractions, and Schwappach et al. (46) found that Gef1p (the only yeast ClC Cl^- channel) localizes to the Golgi. Additionally, elimination of Gef1p from yeast does result in altered cation homeostasis (17) but does not effect Kar2p secretion or glycosylation of invertase, both dependent on an acidic Golgi (46).

It might be argued that since our experiments were performed on single cells, they are not comparable to those performed on confluent monolayers. We attempted to make pH_G measurements on confluent cells grown on filters, but the background fluorescence con-

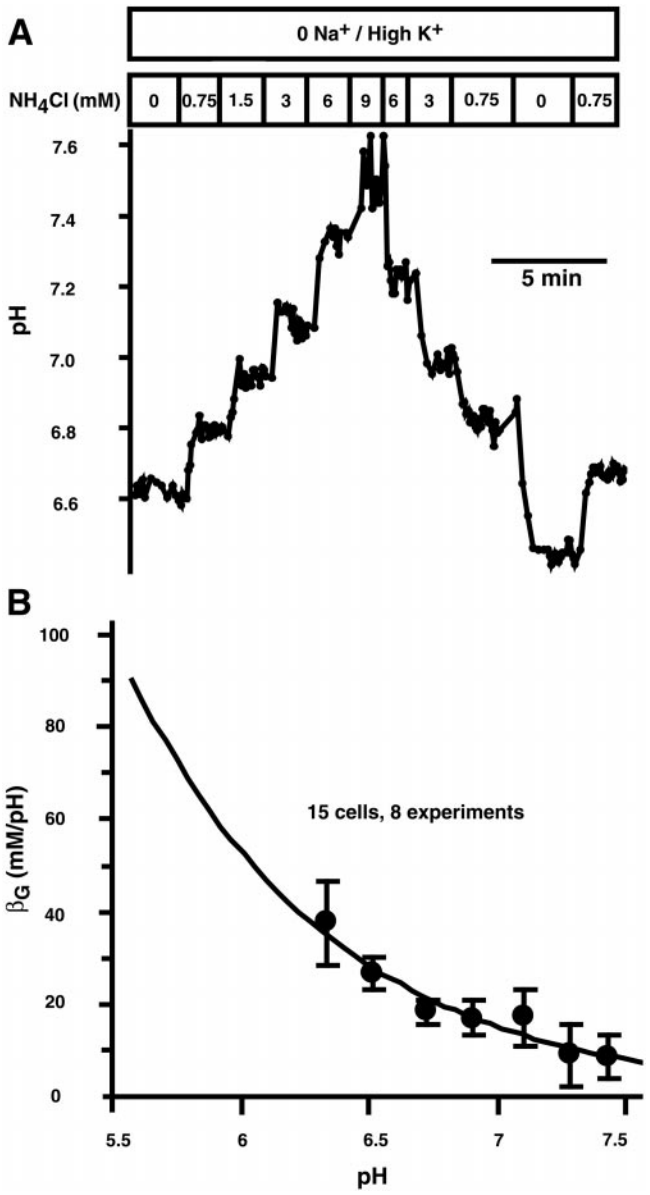

Fig. 7. Golgi buffer capacity (β_G) is pH dependent. *A*: representative trace of 1 cell for which Golgi buffer capacity was obtained. The cell was first acid-loaded with an NH_4Cl prepulse and then exposed to varying amounts of NH_4Cl under Na^+-free/high-K^+ conditions. *B*: summary of all Golgi buffer capacity experiments performed with NH_4Cl and KHOAc. Buffer capacities were grouped by 0.2-pH unit increments. Data are means ± SE. The smooth line is an exponential fit through the data. ($\beta_G = 10.4 \times 10^4\, e^{-1.3\ pH\ units}$).

tributed by the filter exceeded the specific fluorescence of pHERP when excited at 440 and 490 nm under acidic conditions. Therefore, it was impossible to perform experiments when cells were grown on filters. Because of technical difficulties, we were able to obtain only one pH_G measurement from a CFT1-CFTR cell in a confluent patch. Results from this experiment clustered with most of the other CFT1-CFTR data (Fig. 8*C*). We also note that CFTR transits through the Golgi and becomes functional in the plasma membrane of a variety of cells grown on glass either as single cells or in confluent patches (14, 15). We therefore believe, but have not proven, that pH_G experiments performed on isolated cells grown on glass reflect those of confluent cells.

Roles of H^+ Pump, pH-Dependent Leak, and pH_C in Determining pH_G

It has been proposed that pH of the Golgi and other organelles in the secretory pathway is determined primarily by a balance between the active accumulation of protons by the H^+ V-ATPase and the passive loss of H^+ through leaks (10, 61) and that the flux of protons is balanced at pH_G (13). The previous work has not accurately distinguished between effects of the pH gradient and the P_{H^+} in determining H^+ fluxes across the Golgi. Farinas and Verkman (13) showed that as pH_G decreased, the passive H^+ flux out of the Golgi increased. Regardless of the true nature of the H^+ leak pathway, this is not a surprising finding because as the luminal $[H^+]$ is increased, the efflux rate will most probably increase. The present work has extended these conclusions by estimating P_{H^+} and showing that this permeability decreased as pH decreased. We also showed that Golgi buffer capacity was approximately equal to, and showed a pH dependency similar to, that of the cytosol (see Refs. 58 and 59), which supports the assumption that β_G is pH sensitive (42).

As summarized in Fig. 8*C*, P_{H^+} in Golgi of CFT1 cells was $\sim 7.5 \times 10^{-4}$ cm/s when pH_G was 6.5, and there was little difference to CFTR-corrected CFT1 cells. Similar values for Golgi P_{H^+} of HeLa, Vero, and CHO cells were calculated using our model (*Eqs. 2–4*), and bafilomycin-induced alkalinization data were obtained from the literature (Table 2). These P_{H^+} values are large compared with typical permeability values for Na^+, K^+, and Cl^-: 10^{-12} cm/s for a membrane without channels (37) and up to 10^{-5} cm/s for a membrane with channels (22, 24). However, our estimates of P_{H^+} compare favorably with P_{H^+} in lipid bilayers and liposomes: 10^{-7}-10^{-2} cm/s (8, 21, 37, 40). Similar to the data presented for P_{H^+} of the Golgi, artificial lipid bilayers also have pH-dependent P_{H^+} (8, 21). It therefore seems possible that P_{H^+} of the Golgi might be solely due to simple H^+ diffusion through membranes, and variations in P_{H^+} could therefore be due to differences in fatty acids (which act as weak acid shuttles) and/or lipids (which can form water "wires") (8, 20, 21) in the Golgi of different cells. In addition, H^+ channels may also provide leak pathways for H^+ in the Golgi (43). However, estimates of $P_{H^+} > 5 \times 10^{-1}$ cm/s for plasma membranes of lung alveolar cells with H^+ channels [using GHK, reported pH gradients, and measured current densities (6, 9)] was 100 times larger than the largest P_{H^+} observed in the present experiments. Finally, Na^+/H^+ exchange in the Golgi might contribute to the H^+ permeability. However, Schapiro and Grinstein (43) showed that NHEs play no role in the efflux of H^+ from the Golgi. Also, we have found that treatment of CFT1 cells with hexamethylene

amiloride (membrane-permeant analog of amiloride) had no effect on steady-state pH_G (data not shown).

A consequence of the Golgi having a relatively large, pH-dependent P_{H^+} is that pH_G will be a complicated function of pH_C, P_{H^+}, and H^+ pumping. The role of pH_C in determining pH_G is shown by experiments in which cells were treated with NH_3/NH_4^+ and both cytosol and Golgi were first alkalinized and then secondarily acidified (Figs. 3 and 6). Because this secondary acidification also occurred in the presence of bafilomycin (Fig. 5) and thus was not due to the H^+ V-ATPase (as proposed in Refs. 27 and 42), it may have been due to H^+ (or NH_4^+) accumulation across the plasma membrane into the cytosol, which then equilibrated with the Golgi. When extracellular Na^+ was added back to acidified cells, the Golgi alkalinized at a rate that was only 2.5-fold slower than that of the cytosol, likely due to a delayed leak of H^+ from the Golgi into the cytosol, which was being alkalinized due to active H^+ extrusion by NHE in the plasma membrane.

The role of H^+ pumps in setting pH_G was suggested by the fact that HeLa cells had a more acidic Golgi than respiratory epithelial cells (Table 1). This was not solely due to the more acidic pH_C in HeLa cells because the Golgi-to-cytosol $[H^+]$ gradient was larger in HeLa (3.6×10^{-7} M) than in respiratory epithelial cells ($0.75–1.7 \times 10^{-7}$ M) (Table 1). Given that P_{H^+} of HeLa and other cells was similar in the pH 6.4–6.6 range (Fig. 8*C*), the most likely explanation is a difference in H^+-pump activity between HeLa cells and CFT1 cells. This explanation would also apply to the difference between pH_G of CFT1 and CFT1-CFTR cells, although why or how various pump activities would arise in different cells is not clear.

A potential regulatory role for the H^+ pump has been considered previously by Kim et al. (27), who found that pH_G was constant in the face of altered pH_C. In contrast, the present data show that when pH_C was acidified from an average of 7.5 to 6.5, pH_G acidified on average from 6.5 to 6.2. These averages predict that the Golgi-to-cytosol $[H^+]$ gradient is constant in the face of an apparently decreasing P_{H^+} and constant H^+ pump. It will be necessary to measure pH_C and pH_G in the same cells to determine whether H^+ pump and leak may be regulated. It also will be important to determine the roles of pH_C, H^+ pump, and pH-dependent H^+ leak in generating the wide range of pH values

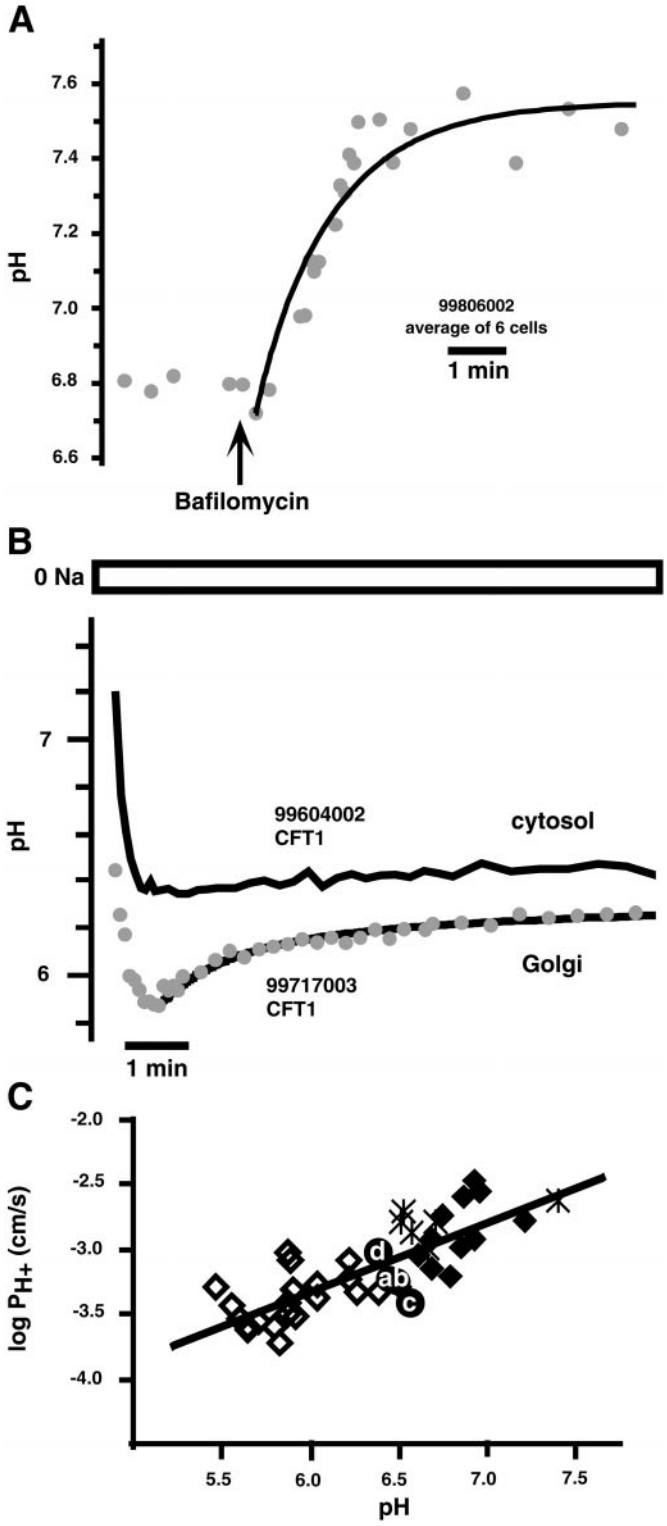

Fig. 8. P_{H^+} is pH dependent. *A*: representative trace showing that when cells were treated with bafilomycin, pH_G rapidly alkalinized. Data from the average of 6 cells are represented by points. The smooth line is the best fit of the data obtained from *Eqs. 2–4* with the pumps turned off. *B*: superimposition of pH_G (Golgi) and pH_C (cytosol) traces after compartments were acid loaded (as in Fig. 6, *A* and *B*). Notice that on this time scale pH_C was relatively constant, while pH_G recovered. Golgi pH (data points) was fit using *Eqs. 2–4* (smooth line). At ~7 min, the average gradient returned to 2.0×10^{-7} M. *C*: log P_{H^+} plotted against pH_G. Filled diamonds represent data from bafilomycin-treated CFT1 cells as described in Fig. 7*A*. Asterisks represent data from bafilomycin-treated CFT1-CFTR cells (1 CFT1-CFTR in the cluster of 5 was a cell from a confluent patch). Open diamonds represent acid-loaded cells that were not treated with bafilomycin, as in Fig. 7*B*. Open circles (*a–d*) represent values extrapolated from the literature (see Table 2). The smooth line is a linear regression through the CFT1 data where $\log P_{H^+} = 0.53\ pH - 6.50$. The slope of the line is significantly different from a line with a slope of zero ($P < 0.01$). Data from the literature and CFT1-CFTR cells were not included in the linear regression.

found in other acidic organelles [e.g., endosomes (pH 6.0–6.5), lysosomes (pH 4–5), and secretory granules (pH 4–5)] in different cells.

We thank Minnie Wu for useful discussions and for providing measurements of average pH_C for HeLa cells. We thank Eric Wunderlich for providing measurements of average pH_C for JME cells.

This work was supported by National Institute of Diabetes and Digestive and Kidney Diseases Grant DK-51799 (to T. Machen), and grants from Cystic Fibrosis Research, Inc. (to G. Chandy and H.-P. H. Moore). M. Grabe was supported by National Science Foundation Grant DMS9220719 (to George Oster, whom we thank for useful discussions).

Present address of G. Chandy: Dept. of Molecular Pharmacology, Stanford, CA 94305-5175.

REFERENCES

1. **Al-Awqati Q, Barasch J, and Landry D.** Chloride channels of intracellular organelles and their potential role in cystic fibrosis. *J Exp Biol* 172: 245–266, 1992.
2. **Barasch J, Kiss B, Prince A, Saiman L, Gruenert D, and al-Awqati Q.** Defective acidification of intracellular organelles in cystic fibrosis. *Nature* 352: 70–73, 1991.
3. **Breen KC and Regan CM.** Developmental control of N-CAM sialylation state by Golgi sialyltransferase isoforms. *Development* 104: 147–154, 1988.
4. **Busam K and Decker K.** Ganglioside biosynthesis in rat liver. Characterization of three sialyltransferases. *Eur J Biochem* 160: 23–30, 1986.
5. **Cheng PW, Boat TF, Cranfill K, Yankaskas JR, and Boucher RC.** Increased sulfation of glycoconjugates by cultured nasal epithelial cells from patients with cystic fibrosis. *J Clin Invest* 84: 68–72, 1989.
6. **Cherny VV, Markin VS, and DeCoursey TE.** The voltage-activated hydrogen ion conductance in rat alveolar epithelial cells is determined by the pH gradient. *J Gen Physiol* 105: 861–896, 1995.
7. **Davies JM, Hunt I, and Sanders D.** Vacuolar H^+-pumping ATPase variable transport coupling ratio controlled by pH. *Proc Natl Acad Sci USA* 91: 8547–8551, 1994.
8. **Deamer DW.** Proton permeation of lipid bilayers. *J Bioenerg Biomembr* 19: 457–479, 1987.
9. **DeCoursey TE and Cherny VV.** Voltage-activated hydrogen ion currents. *J Membr Biol* 141: 203–223, 1994.
10. **Demaurex N, Furuya W, D'Souza S, Bonifacino JS, and Grinstein S.** Mechanism of acidification of the trans-Golgi network (TGN). In situ measurements of pH using retrieval of TGN38 and furin from the cell surface. *J Biol Chem* 273: 2044–2051, 1998.
11. **Dosanjh A, Lencer W, Brown D, Ausiello DA, and Stow JL.** Heterologous expression of ΔF508 CFTR results in decreased sialylation of membrane glycoconjugates. *Am J Physiol Cell Physiol* 266: C360–C366, 1994.
12. **Dunn KW, Park J, Semrad CE, Gelman DL, Shevell T, and McGraw TE.** Regulation of endocytic trafficking and acidification are independent of the cystic fibrosis transmembrane regulator. *J Biol Chem* 269: 5336–5345, 1994.
13. **Farinas J and Verkman AS.** Receptor-mediated targeting of fluorescent probes in living cells. *J Biol Chem* 274: 7603–7606, 1999.
14. **Fischer H, Illek B, and Machen T.** Regulation of CFTR by protein phosphatase 2B and protein kinase C. *Pflügers Arch* 436: 175–181, 1998.
15. **Fischer H, Kreusel K, Illek B, Machen T, Hegel U, and Clauss W.** The outwardly rectifying Cl^- channel is not involved in cAMP-mediated Cl. *Pflügers Arch* 422: 159–167, 1992.
16. **Freischutz B, Saito M, Rahmann H, and Yu RK.** Characterization of sialyltransferase-IV activity and its involvement in the c-pathway of brain ganglioside metabolism. *J Neurochem* 64: 385–393, 1995.
17. **Gaxiola R, Yuan D, Klausner R, and Fink G.** The yeast CLC chloride channel functions in cation homeostasis. *Proc Natl Acad Sci USA* 95: 4046–4050, 1998.
18. **Grabe M and Oster G.** Regulation of organelle acidity. *J Gen Physiol* 117: 329–344, 2001.
19. **Grabe M, Wang H, and Oster G.** The mechanochemistry of V-ATPase proton pumps. *Biophys J* 78: 2798–2813, 2000.
20. **Gutknecht J.** Proton conductance caused by long-chain fatty acids in phospholipid bilayer membranes. *J Membr Biol* 106: 83–93, 1988.
21. **Gutknecht J.** Proton conductance through phospholipid bilayers: water wires or weak acids? *J Bioenerg Biomembr* 19: 427–442, 1987.
22. **Hartmann T and Verkman AS.** Model of ion transport regulation in chloride-secreting airway epithelial cells. Integrated description of electrical, chemical, and fluorescence measurements. *Biophys J* 58: 391–401, 1990.
23. **Hille B.** *Ionic channels of excitable membranes*. Sunderland, MA: Sinauer, 1992.
24. **Huflejt ME, Blum RA, Miller SG, Moore HP, and Machen TE.** Regulated Cl transport, K and Cl permeability, and exocytosis in T84 cells. *J Clin Invest* 93: 1900–1910, 1994.
25. **Imundo L, Barasch J, Prince A, and Al-Awqati Q.** Cystic fibrosis epithelial cells have a receptor for pathogenic bacteria on their apical surface *Proc Natl Acad Sci USA* 92: 3019–3023, 1995. [Corrigenda. *Proc Natl Acad Sci USA* 92: November 1995, p. 11322.]
26. **Kim JH, Johannes L, Goud B, Antony C, Lingwood CA, Daneman R, and Grinstein S.** Noninvasive measurement of the pH of the endoplasmic reticulum at rest and during calcium release. *Proc Natl Acad Sci USA* 95: 2997–3002, 1998.
27. **Kim JH, Lingwood CA, Williams DB, Furuya W, Manolson MF, and Grinstein S.** Dynamic measurement of the pH of the Golgi complex in living cells using retrograde transport of the verotoxin receptor. *J Cell Biol* 134: 1387–1399, 1996.
28. **Kneen M, Farinas J, Li Y, and Verkman AS.** Green fluorescent protein as a noninvasive intracellular pH indicator. *Biophys J* 74: 1591–1599, 1998.
29. **Kunzelmann K, Kathofer S, and Greger R.** Na^+ and Cl^- conductances in airway epithelial cells: increased Na^+ conductance in cystic fibrosis. *Pflügers Arch* 431: 1–9, 1995.
30. **Ladinsky MS, Mastronarde DN, McIntosh JR, Howell KE, and Staehelin LA.** Golgi structure in three dimensions: functional insights from the normal rat kidney cell. *J Cell Biol* 144: 1135–1149, 1999.
31. **Lee MG, Choi JY, Luo X, Strickland E, Thomas PJ, and Muallem S.** Cystic fibrosis transmembrane conductance regulator regulates luminal Cl^-/HCO_3^- exchange in mouse submandibular and pancreatic ducts. *J Biol Chem* 274: 14670–14677, 1999.
32. **Llopis J, McCaffery JM, Miyawaki A, Farquhar MG, and Tsien RY.** Measurement of cytosolic, mitochondrial, and Golgi pH in single living cells with green fluorescent proteins. *Proc Natl Acad Sci USA* 95: 6803–6808, 1998.
33. **Lukacs GL, Chang XB, Kartner N, Rotstein OD, Riordan JR, and Grinstein S.** The cystic fibrosis transmembrane regulator is present and functional in endosomes. Role as a determinant of endosomal pH. *J Biol Chem* 267: 14568–14572, 1992.
34. **Miesenbock G, De Angelis DA, and Rothman JE.** Visualizing secretion and synaptic transmission with pH-sensitive green fluorescent proteins. *Nature* 394: 192–195, 1998.
35. **Nordeen M, Jones S, Howell K, and Caldwell J.** GOLAC: an endogenous anion channel of the Golgi complex. *Biophys J* 78: 2918–2928, 2000.
36. **Ostrander GK and Holmes EH.** Characterization of a CMP-NeuAc: lactosylceramide alpha2—-3sialyltransferase from rainbow trout hepatoma (RTH-149) cells. *Comp Biochem Physiol B* 98: 87–95, 1991.
37. **Paula S, Volkov AG, Van Hoek AN, Haines TH, and Deamer DW.** Permeation of protons, potassium ions, and small polar molecules through phospholipid bilayers as a function of membrane thickness. *Biophys J* 70: 339–348, 1996.

38. **Press WH.** *Numerical recipes in C: the art of scientific computing*. Cambridge, UK: Cambridge Univ. Press, 1997.
39. **Reddy MM, Light MJ, and Quinton PM.** Activation of the epithelial Na^+ channel (ENaC) requires CFTR Cl^- channel function. *Nature* 402: 301–304, 1999.
40. **Rivers R, Blanchard A, Eladari D, Leviel F, Paillard M, Podevin RA, and Zeidel ML.** Water and solute permeabilities of medullary thick ascending limb apical and basolateral membranes. *Am J Physiol Renal Physiol* 274: F453–F462, 1998.
41. **Roos A and Boron WF.** Intracellular pH. *Physiol Rev* 61: 296–434, 1981.
42. **Schapiro F, Sparkowski J, Adduci A, Suprynowicz F, Schlegel R, and Grinstein S.** Golgi alkalinization by the papillomavirus E5 oncoprotein. *J Cell Biol* 148: 305–315, 2000.
43. **Schapiro FB and Grinstein S.** Determinants of the pH of the Golgi complex. *J Biol Chem* 275: 21025–21032, 2000.
44. **Schapiro FB, Lingwood C, Furuya W, and Grinstein S.** pH-independent retrograde targeting of glycolipids to the Golgi complex. *Am J Physiol Cell Physiol* 274: C319–C332, 1998.
45. **Schroeder TH, Zaidi T, and Pier GB.** Lack of adherence of clinical isolates of *Pseudomonas aeruginosa* to Asialo-GM(1) on epithelial cells. *Infect Immun* 69: 719–729, 2001.
46. **Schwappach B, Stobrawa S, Hechenberger M, Steinmeyer K, and Jentsch T.** Golgi localization and functionally important domains in the NH_2 and COOH terminus of the yeast CLC putative chloride channel Gef1p. *J Biol Chem* 273: 15110–15118, 1998.
47. **Seed B and Aruffo A.** Molecular cloning of the CD2 antigen, the T-cell erythrocyte receptor, by a rapid immunoselection procedure. *Proc Natl Acad Sci USA* 84: 3365–3369, 1987.
48. **Seksek O, Biwersi J, and Verkman AS.** Direct measurement of trans-Golgi pH in living cells and regulation by second messengers. *J Biol Chem* 270: 4967–4970, 1995.
49. **Seksek O, Biwersi J, and Verkman AS.** Evidence against defective trans-Golgi acidification in cystic fibrosis. *J Biol Chem* 271: 15542–15548, 1996.
50. **Stutts MJ, Canessa CM, Olsen JC, Hamrick M, Cohn JA, Rossier BC, and Boucher RC.** CFTR as a cAMP-dependent regulator of sodium channels. *Science* 269: 847–850, 1995.
51. **Taga R, Alvares EP, and Sesso A.** Morphometric studies on terminal tubule and acinar cells in developing submandibular gland of the rat. *Arch Histol Cytol* 56: 517–523, 1993.
52. **Tang BL, Low SH, Wong SH, and Hong W.** Cell type differences in Golgi retention signals for transmembrane proteins. *Eur J Cell Biol* 66: 365–374, 1995.
53. **Teruel MN, Blanpied TA, Shen K, Augustine GJ, and Meyer T.** A versatile microporation technique for the transfection of cultured CNS neurons. *J Neurosci Methods* 93: 37–48, 1999.
54. **Teter K, Chandy G, Quinones B, Pereyra K, Machen T, and Moore HP.** Cellubrevin-targeted fluorescence uncovers heterogeneity in the recycling endosomes. *J Biol Chem* 273: 19625–19633, 1998.
55. **Tsien RY.** The green fluorescent protein. *Annu Rev Biochem* 67: 509–544, 1998.
56. **Van Dyke R and Belcher J.** Acidification of three types of liver endocytic vesicles: similarities and differences. *Am J Physiol Cell Physiol* 266: C81–C94, 1994.
57. **Wachter RM and Remington SJ.** Sensitivity of the yellow variant of green fluorescent protein to halides and nitrate. *Curr Biol* 9: R628–R629, 1999.
58. **Weintraub WH and Machen TE.** pH regulation in hepatoma cells: roles for Na-H exchange, Cl-HCO_3 exchange, and Na-HCO3 cotransport. *Am J Physiol Gastrointest Liver Physiol* 257: G317–G327, 1989.
59. **Wenzl E and Machen TE.** Intracellular pH dependence of buffer capacity and anion exchange in the parietal cell. *Am J Physiol Gastrointest Liver Physiol* 257: G741–G747, 1989.
60. **Wong SH, Low SH, and Hong W.** The 17-residue transmembrane domain of beta-galactoside α2,6-sialyltransferase is sufficient for Golgi retention. *J Cell Biol* 117: 245–258, 1992.
61. **Wu MM, Llopis J, Adams S, McCaffery JM, Kulomaa MS, Machen TE, Moore HPH, and Tsien RY.** Organelle pH studies using targeted avidin and fluorescein-biotin. *Chem Biol* 7: 197–209, 2000.
62. **Yankaskas JR, Haizlip JE, Conrad M, Koval D, Lazarowski E, Paradiso AM, Rinehart CA Jr, Sarkadi B, Schlegel R, and Boucher RC.** Papilloma virus immortalized tracheal epithelial cells retain a well-differentiated phenotype. *Am J Physiol Cell Physiol* 264: C1219–C1230, 1993.
63. **Zar H, Saiman L, Quittell L, and Prince A.** Binding of *Pseudomonas aeruginosa* to respiratory epithelial cells from patients with various mutations in the cystic fibrosis transmembrane regulator. *J Pediatr* 126: 230–233, 1995.